

UC Berkeley

UC Berkeley Previously Published Works

Title

Competitive sorption of microbial metabolites on an iron oxide mineral

Permalink

<https://escholarship.org/uc/item/3z09f7hd>

Authors

Swenson, Tami L
Bowen, Benjamin P
Nico, Peter S
[et al.](#)

Publication Date

2015-11-01

DOI

10.1016/j.soilbio.2015.07.022

Peer reviewed

1
2
3
4
5
6
7
8
9
10
11
12
13
14
15
16
17
18
19
20
21
22
23

Competitive sorption of microbial metabolites on an iron oxide mineral

Tami L. Swenson¹, Benjamin P. Bowen¹, Peter S. Nico², Trent R. Northen^{1*}

¹Life Sciences Division, Lawrence Berkeley National Laboratory, 1 Cyclotron Road, Berkeley, CA 94720, USA

²Earth Sciences Division, Lawrence Berkeley National Laboratory, 1 Cyclotron Road, Berkeley, CA 94720, USA

**Corresponding author: E-mail: TRNorthen@lbl.gov; Fax: +1 (510) 486-4545; Tel: +1 (510) 486-5240*

24 **ABSTRACT**

25 A large fraction of soil organic matter (SOM) is composed of small molecules of
26 microbial origin. However, the biotic and abiotic cycling of these nutrients is poorly understood
27 and is a critical component of the global carbon cycle. Although there are many factors
28 controlling the accessibility of SOM to microbes, sorption to mineral surfaces is among the most
29 significant. Here, we investigated the competitive sorption of a complex pool of microbial
30 metabolites on ferrihydrite, an iron oxide mineral, using a lysate prepared from a soil bacterium,
31 *Pseudomonas stutzerii* RCH2. After a 24-hour incubation with a range of mineral concentrations,
32 more than half of the metabolites showed significant decreases in solution concentration.
33 Phosphate-containing metabolites showed the greatest degree of sorption followed by
34 dicarboxylates and metabolites containing both nitrogen and an aromatic moiety. Similar trends
35 were observed when comparing sorption of metabolites with an equimolar metabolite mixture
36 rather than a bacterial lysate. Interestingly, ectoine, lysine, two disaccharides and uracil were
37 found not to sorb and may be more bioavailable in iron oxide-rich soils. Additionally, the
38 highest-sorbing metabolites were examined for their ability to mobilize mineral-sorbed
39 phosphate. All phosphate-containing metabolites tested and glutathione released phosphate from
40 the mineral surface within 30 minutes of metabolite addition. These findings of preferential
41 sorption behavior within a complex pool of microbial metabolites may provide insight into the
42 cycling of SOM and specific nutrient availability. Finally, the release of highly-sorptive
43 metabolites may be an underexplored mechanism utilized by microbial communities to gain
44 access to limited environmental nutrients.

45

46 **Keywords:** ferrihydrite, sorption, phosphate, soil organic matter, metabolomics

47 **1. INTRODUCTION**

48 Terrestrial ecosystems store more carbon than plant biomass and the atmosphere
49 combined with soil organic matter (SOM) being the largest terrestrial pool of organic carbon
50 (Batjes, 1996; Houghton, 2007). Many contradictory predictions exist regarding the effects
51 climate change will have on microbial activity and composition and the role terrestrial
52 ecosystems will play in the overall carbon cycle (Davidson and Janssens, 2006; Giardina and
53 Ryan, 2000; Hopkins et al., 2012; Karhu et al., 2014). A critical step toward developing better
54 terrestrial carbon cycling models is to understand not only the chemical composition of SOM,
55 but factors controlling the stability, behavior and (microbial) accessibility of these compounds.
56 This may ultimately allow us to predict climate-induced alterations in microbial community
57 composition and anticipate changes in carbon mineralization and respiration rates.

58 SOM is a complex mixture of compounds with a large fraction derived from microbial
59 products (Ludwig et al., 2015; Schmidt et al., 2011). The soluble fraction (dissolved organic
60 matter, DOM) accounts for less than 2% of SOM, but is the most accessible fraction for
61 microbial degradation and therefore DOM turnover is likely an accurate representation of overall
62 SOM cycling (Guigue et al., 2015; Kaiser and Kalbitz, 2012; Kalbitz, 2003). Subsoil DOM
63 consists of microbial products (Kaiser and Kalbitz, 2012), but the specific chemical composition
64 of DOM is just beginning to be more thoroughly characterized and includes carbohydrates,
65 amino acids, organic acids, fatty acids, sterols and nucleosides (Kakumanu et al., 2013; Swenson
66 et al., 2015; Warren, 2015). Microbes rely on DOM as an important carbon source and tend to
67 prefer carbohydrates and amino acids over complex (possibly lignin-derived) aromatic molecules
68 (Amon et al., 2001; Kalbitz, 2003). As a result of substrate preferences such as these, microbial
69 function and community structure are highly influenced by the abundance and the composition

70 of DOM (Guigue et al., 2015; Heckman et al., 2013a; Hopkinson et al., 1998; Judd et al., 2006).
71 Hence, alteration of the DOM composition can have a drastic affect on microbial community
72 structure.

73 In addition to microbial processing, many abiotic (*e.g.* sorption, precipitation, dissolution,
74 diffusion) processes affect microbial accessibility and overall cycling of DOM (Kaiser and
75 Kalbitz, 2012; Kalbitz et al., 2000; Zsolnay, 1996). Sorption to mineral surfaces is potentially the
76 most impactful abiotic factor. Specific mineral content (clay, iron oxide minerals, *etc*) and
77 surface area have a strong influence on the solid-solution partitioning and the accessibility of
78 DOM components to microorganisms (Kalbitz et al., 2000). It would follow that the sorption
79 behavior of specific metabolites may influence community structure by changing the
80 bioavailability of DOM components favoring microbes that can best utilize the available
81 components and access adsorbed metabolites. Indeed, recent studies show that soil composition,
82 in terms of mineral and clay content, shapes microbial community structure (Heckman et al.,
83 2013b; Vogel et al., 2014). For example, forest floor DOM sorption dynamics with goethite and
84 gibbsite affect microbial community composition in a time-dependent manner (Heckman et al.,
85 2013b).

86 There are limited studies aimed at examining the sorption behavior of well-characterized
87 DOM components on minerals. However, there is general agreement that iron (hydr)oxide
88 minerals such as goethite, ferrihydrite and hematite preferentially sorb molecules containing
89 aromatic, nitrogen, phosphate and carboxylate groups (Omoike and Chorover, 2006; Yeasmin et
90 al., 2014; Zhou et al., 2001). These strong, and often irreversible, mineral-nutrient interactions
91 have a drastic influence on biological dynamics. While studies such as these have led to our
92 understanding of sorption-based DOM stability of general classes of compounds, in order to link

93 DOM cycling with soil microbial community dynamics, there is a need to investigate specific
94 metabolite sorption behavior.

95 Another essential component of understanding nutrient availability in terrestrial systems
96 is evaluating how mineral sorption of DOM molecules can affect the mobility of vital mineral-
97 restricted nutrients such as phosphorus. Although total phosphorus in soils is generally high,
98 available soluble forms are limited mostly due to phosphate sorption to mineral surfaces,
99 especially iron and aluminum oxides (Arai and Sparks, 2007; Sharma et al., 2013; Wang et al.,
100 2013). Microbes have developed many mechanisms for phosphate mobilization including
101 production of phosphatases, lowering of soil pH and release of organic acids (Sharma et al.,
102 2013). Possibly due to the limited availability of appropriate metabolomics technology,
103 investigations into phosphate mobilization by high-sorbing DOM components, other than
104 organic acids, are limited.

105 The objective of this study was to examine the sorption behavior of microbial metabolites
106 as they exist in a competitive and complex, biologically-relevant mixture. Most studies to date
107 tend to focus either on simple systems (Cagnasso et al., 2010; Persson and Axe, 2005) or
108 complex mixtures of organics that are only roughly characterized (Heckman et al., 2013a; Kaiser
109 and Guggenberger, 2007). We used lysates prepared from a soil bacterium to represent
110 compounds commonly found in DOM. This mixture of microbial metabolites represents a unique
111 system that is both highly complex and well-characterized (Swenson et al., 2015). Aged
112 ferrihydrite, an iron (oxyhydr)oxide mineral, was used as our model sorbent due to its ubiquitous
113 presence in natural systems and its nanoporous, highly reactive and large specific surface area
114 (Heimstra and Riemsdijk, 2009). Metabolite sorption as a function of mineral concentration was
115 monitored by liquid chromatography/ mass spectrometry (LC/MS). Individual high-sorbing

116 compounds were then selected to investigate the potential to desorb and mobilize phosphate from
117 the mineral surface. These data may shed light onto exometabolite mechanisms by soil microbes
118 to gain access to limiting nutrients such as phosphate.

119

120 **2. MATERIALS AND METHODS**

121 **2.1. Materials**

122 LC/MS-grade water and LC/MS-grade methanol (CAS 67-56-1) were from Honeywell
123 Burdick & Jackson (Morristown, NJ). LC/MS-grade OmniSolv acetonitrile (CAS 75-05-8) was
124 from EMD Millipore (Billerica, MA). MOPS (CAS 1132-61-2), HEPES (CAS 7365-45-9), 3,6-
125 dihydroxy-4-methylpyridazine (CAS 5754-18-7), 4-(3,3-dimethyl-ureido)benzoic acid (CAS
126 91880-51-2), d₅-benzoic acid (CAS 1079-02-3), 9-anthracenecarboxylic acid (CAS 723-62-6),
127 ammonium acetate (CAS 631-61-8), KH₂PO₄ (CAS 7778-77-0) were from Sigma (St. Louis,
128 MO). All compounds in the standards mixture were from Sigma (St. Louis, MO).

129 Ferrihydrite was synthesized according to the procedure of Schwertmann and Cornell
130 (2000) and dry-aged in the dark for eight years. The resulting mineral was characterized by x-ray
131 diffraction and shown to be low crystallinity, 2-line ferrihydrite. Bacterial lysates were prepared
132 using the soil isolate, *Pseudomonas stutzeri* RCH2, obtained from Romy Chakraborty (LBNL).
133 Bacteria were grown in M9 minimal media containing sodium acetate (0.2%) as the carbon
134 source and lysates prepared according to the protocol in Swenson et al (2015). In brief, cultures
135 were grown in M9 minimal media until an optical density of 0.5 (at 600 nm) was reached. Cells
136 were pelleted by centrifuging at 3220 x g for 10 min, washed with cold phosphate-buffered
137 saline (pH 7.4) and re-pelleted. The supernatant was discarded and pellets resuspended in 1 mL
138 cold methanol, sonicated for 2 x 20 s using a Q125 QSonica sonicator then 5 min in a sonicating

139 water bath (VWR symphony), centrifuged at 2348 x g for 5 min and the supernatant dried.
140 Lysates were resuspended in sterile LC/MS-grade water resulting in a total organic carbon
141 (TOC) content of 158 mg/L (Shimadzu TOC-V CSH analyzer, Kyoto, Japan), a pH of 6.8 and 55
142 (including six putative) metabolites identified by LC/MS analysis (**Supplementary Table 1**).

143 To explore the relative sorption behavior of bacterial metabolites when present in
144 equimolar concentrations, the ferrihydrite sorption experiment was conducted with an equimolar
145 mixture of standards. Each compound was prepared at 20 μ M each (final concentration) in
146 LC/MS-grade water, resulting in a pH of 6.8. The standards mixture contained 44 out of the 55
147 compounds reported for the bacterial lysates (the remaining 11 compounds were unavailable)
148 plus five additional compounds (nicotinic acid, dodecanoic acid, hydroxy-proline, ornithine,
149 raffinose) that were detected in the preliminary analysis of bacterial lysates (but not included in
150 the final results of that experiment due to small and ambiguous peaks). Maltose and trehalose
151 were included in the mixture to represent disaccharide 1 and 2, respectively. Of the metabolites
152 added, five were not detected (coenzyme A, tyrosine, citramalic acid, glutathione and alanine)
153 indicating that they may be present in higher concentrations in the lysate than in the standards
154 mixture. The TOC of the standards mixture was 1.698 g/L.

155

156 **2.2. Metabolite sorption assay**

157 Resuspended lysates or standards mixture (1 mL) was added to 5 mL Eppendorf tubes
158 containing mineral (0, 0.5, 1, 2, 4, 8, 16 or 32 mg), tilted at 90° and shaken on an orbital shaker
159 (Orbital-Genie, Scientific Industries, Bohemia, NY) at 200 rpm for 24 h at 25°C. For the
160 temperature-effect experiment, samples were shaken for 24 h either at 4°C, 25°C or 37°C.
161 Samples were centrifuged at 3220 x g for 15 minutes and 950 μ L of the supernatant dried down

162 with a Savant SpeedVac SPD111V (Thermo Scientific, Waltham, WA) and resuspended in
163 100% methanol (200 uL for lysates, 300 uL for the standards mixture) containing internal
164 standards (MOPS, HEPES, 3,6-dihydroxy-4-methylpyridazine, 4-(3,3-dimethyl-ureido)benzoic
165 acid, d₅-benzoic acid and 9-anthracene carboxylic acid at 5 µg/mL each). Resuspended samples
166 were vortexed and sonicated for 5 min followed by filtration through 0.22 µm centrifugal
167 membranes (Nanosep MF, Pall Corporation, Port Washington, NY). Each sorption condition
168 contained five replicates.

169

170 **2.3. LC/MS analysis**

171 Extracts were analyzed using normal phase liquid chromatography with a ZIC-pHILIC
172 column (150 mm × 2.1 mm, 3.5 µm 200 Å, Merck Sequant, Darmstadt, Germany) using an
173 Agilent 1290 series UHPLC (Agilent Technologies, Santa Clara, California, USA) with an
174 Agilent 6550 quadropole time-of-flight mass spectrometer using both positive and negative
175 polarities. Samples were maintained at 4°C prior to injection. Mobile phase for chromatographic
176 separation was A: 5mM ammonium acetate and B: 90% acetonitrile w/ 5mM ammonium acetate.
177 Upon sample injection, initial conditions of 100% B at a flow rate of 0.25 mL/min were held for
178 1.5 min after which the following gradient was applied: linear decrease to 50% B at 25 min; hold
179 until 29.9 min, return to initial conditions at 30 min with a total runtime of 40 min for column re-
180 equilibration. Column temperature was maintained at 40°C. Flow was directed to the
181 electrospray MS source which was operated at the following setpoints for both positive and
182 negative polarity ionization: drying gas temperature and flow: 275°C and 14 L/min; sheath gas
183 temperature and flow: 275°C and 9 L/min; nebulizer pressure: 30 psi; capillary voltage: 3500 V;
184 nozzle voltage: 1000 V. Mass spectra were acquired from 50-1700 m/z at 4 spectra s⁻¹.

185

186 **2.4. Data analysis**

187 Data were analyzed using Metabolite Atlas (Bowen et al, 2015) and the Python
188 programming language. Metabolite identification was based on two orthogonal data relative to
189 authentic standards: exact mass (± 5 ppm) and retention time (± 60 s) in accordance with the
190 metabolomics reporting standards (Sumner et al, 2007). Putative identifications were assigned in
191 the cases where authentic standards were not available (and indicated in figures by parentheses).
192 Instrument performance was monitored by including internal standards in each sample and by
193 running a quality control mixture before and after each sample set. Metabolites were not
194 quantified since the focus of this study was on the sorption behavior of individual metabolites
195 relative to each other in a biologically-relevant ratio (for the bacterial lysates experiment) and
196 relative to non-mineral controls. Instead, peak areas for each metabolite were compared across
197 all samples and sorption results are reported as a percentage (peak area) of the non-mineral
198 control. To determine statistical significance between mineral-containing samples and the
199 control, peak areas were log₂ transformed and a two-way ANOVA was performed along with
200 the Dunnett's test to correct for multiple comparisons. A *p* value less than 0.05 was considered
201 significant. These calculations only reflect significance between metabolite peak areas with and
202 without mineral.

203

204 **2.5. Phosphate release assay**

205 Phosphate desorption from mineral was measured by loading the mineral (10 mg) with
206 phosphate (10 mL of 0.25 mM KH₂PO₄, pH 7) by shaking on an orbital shaker at 200 rpm for 24
207 h at 25°C. At the end of the phosphate loading step, an aliquot (500 μ L) was removed to measure

208 phosphate concentrations. To pellet the mineral (containing sorbed phosphate), samples were
209 centrifuged at 3220 x g for 15 minutes and the supernatant discarded. Mineral pellets were
210 resuspended in metabolite solution (10 mL of 2.5 mM metabolite in deionized water, pH 7) and
211 shaken as above for 24 h. A metabolite-free control (deionized water) was included to account
212 for the amount of phosphate released from the pellet during the 24 h incubation. Aliquots (500
213 μL) were removed 30 min, 60 min, 120 min and 24 h following metabolite addition. Phosphate
214 concentrations were measured in the initial KH_2PO_4 solution, 24 h post-phosphate loading and
215 the above timepoints post-metabolite addition using the phosphate colorimetric kit (Sigma-
216 Aldrich, Saint Louis, MO). Each aliquot used for phosphate measurement was cleared of solid
217 phase by centrifuging at 10,000 x g for 10 min, plated (20 μL) on a clear 96-well flat-bottom
218 plate with deionized water (180 μL) and phosphate colorimetric reagent (30 μL) and mixed by
219 pipetting. The plate was incubated at room temperature in the dark for 30 min and absorbance
220 read at 650 nm. The background absorbance for each metabolite solution was measured before
221 and after 24 h on the orbital shaker. Each sorption experiment was performed in triplicate. The
222 initial amount of phosphate assumed to be bound to the mineral after the 24 h loading phase was
223 calculated by:

$$224 \quad P_S(24) = A_{650}(\text{initial}) - A_{650}(24\text{h})$$

225 where $P_S(24)$ is the phosphate (absorbance potential) bound to mineral after 24 h, $A_{650}(\text{initial})$ is
226 the absorbance at 650 nm of the initial KH_2PO_4 solution and $A_{650}(24\text{h})$ is the absorbance of the
227 KH_2PO_4 solution after the 24 h loading phase. The percent phosphate desorption was then
228 calculated by:

$$229 \quad P_D(t) = [A_{650}(t) - A_{650}(0)] / P_S(24\text{h})$$

230 where P_D is the percent phosphate desorbed as a function of time, $A_{650}(t)$ is the absorbance as
231 described above at a given time point, $A_{650}(0)$ is the absorbance of the metabolite solution
232 without added mineral or phosphate, and $P_S(24h)$ is the initial amount of sorbed phosphate.

233

234 **3. RESULTS**

235 ***3.1. Microbial metabolite sorption on solid phase***

236 Iron oxide mineral sorption of microbial metabolites (24 h) was investigated with a series
237 of mineral concentrations to encompass a range of mineral:TOC ratios that may exist in natural
238 systems. The metabolite-mineral incubation did not significantly affect the pH of the solutions,
239 which started at 6.8 and after the 24-h incubation ranged from 6.2-7.2 (varying from sample to
240 sample with no obvious trends with mineral concentration). The detected bacterial metabolites
241 included a broad range of compounds commonly found in SOM (Alexander, 1977). The relative
242 aqueous concentration (calculated as a percentage of the non-mineral control) was significantly
243 decreased by the presence of mineral phase for 32 out of the 55 detected metabolites (reaching at
244 least 76% sorption) (**Figure 1, Supplementary Table 2**). Metabolites were grouped into five
245 categories based on the presence of sorption-associated structural moieties: 1) phosphate-
246 containing, 2) dicarboxylates, 3) both aromatic and N-containing, 4) both carboxylate- and N-
247 containing and 5) other. For all metabolites, sorption occurred in a mineral concentration-
248 dependent manner (sorption increased with the ratio of mineral:TOC) (**Figure 1**). The most
249 sorptive group was the phosphate-containing compounds. All peak areas within this group were
250 significantly decreased by the presence of mineral surface with 100% sorption occurring at an
251 approximate ratio of 50:1 (w/w) (mineral:TOC). The second most sorptive group was the
252 dicarboxylates (all metabolites with significantly decreased solution concentration) followed by

253 the aromatic and N-containing group (10 out of 16 metabolites showed significantly decreased
254 solution concentrations). Only a few metabolites did not sorb at all under the conditions tested:
255 ectoine, lysine, disaccharide 1 and 2 (possibly maltose and trehalose) and uracil. Finally, the
256 overall sorption trends were not affected by temperature (*i.e.* 4°C, 25°C and 37°C) with the
257 phosphate-containing compounds as the most sorptive (**Supplementary Results,**
258 **Supplementary Figure 1**).

259

260 **3.2. Bacterial lysates versus the standards mixture**

261 Since the absolute concentration of each metabolite from the bacterial lysate was not
262 measured, the same experiment was conducted with a mixture of standards in equimolar
263 concentration (20 µM each) to explore the possibility that the sorption behavior was a function of
264 relative abundance of each metabolite within the bacterial lysates. In total, 44 compounds were
265 measured for sorption. It is important to note that the standards mixture contained almost ten
266 times more TOC than the lysates, but the same range of mineral concentrations as in the first
267 experiment was still tested to examine the sorption behavior of each metabolite as a function of
268 increasing mineral concentration. Overall, metabolites in the standards mixture behaved similarly
269 to the bacterial lysates with the phosphate-containing compounds being the most sorptive group
270 (all decreased significantly) (**Figure 2**). Peak areas were significantly reduced by the presence of
271 mineral (reaching at least 78% sorption) for 18 out of the 44 compounds tested (**Figure 2,**
272 **Supplementary Table 2**). In general, the high-sorbing compounds reached 100% sorption
273 (relative to the non-mineral control for each metabolite) at lower mineral:TOC ratios in the
274 standards mixture compared to the bacterial lysates (*e.g.* phosphate-containing compounds,
275 aspartate, glutamate and succinate). Compounds that did not sorb (but did appreciably in the

276 bacterial lysates) were 2'-deoxyuridine and 5-methylthioadenosine. These differences may be a
277 result of these compounds being more abundant in the standards mixture compared to bacterial
278 lysates based on comparison of peak areas (although absolute quantities of the metabolites were
279 not measured).

280

281 ***3.3. Phosphate desorption from the mineral surface***

282 A subset of the most sorptive metabolites was analyzed for their ability to desorb
283 phosphate from the mineral surface. After a 24-h phosphate-loading period, on average, 75% of
284 the added phosphate was sorbed to the mineral surface. Once metabolites were added, those that
285 released the most phosphate (more than 10%) over a period of 24 h included most of the
286 phosphate-containing compounds tested (inosine monophosphate, cytidine monophosphate,
287 adenosine monophosphate, uridine monophosphate, glucose 6-phosphate) and the positive
288 control, citrate (not used in our microbial lysate sorption experiments, but shown in previous
289 studies to desorb phosphate (Johnson and Loeppert, 2006)) (**Figure 3**). Others that resulted in
290 detectable phosphate release, but less than 10%, were glutathione and some phosphate-
291 containing metabolites, NADH, coenzyme A and FAD while fumarate, raffinose, adenosine and
292 5-methylthioadenosine did not cause significant phosphate desorption (**Figure 3**). It is very
293 interesting to note the wide range of phosphate desorption caused by phosphate-containing
294 metabolites. Not all of the phosphate-containing metabolites were highly efficient in releasing
295 phosphate. Deionized water was included as a control and did not release detectable amounts of
296 phosphate, verifying that phosphate release from other samples was metabolite-dependent.

297

298 **4. DISCUSSION**

299 **4.1. Mechanisms of metabolite sorption**

300 The focus of this study was on the sorption behavior of low molecular weight soil
301 bacterium compounds (and only those detectable with our LC/MS method and analysis) rather
302 than on high molecular weight compounds or polymers. The undetected metabolites and larger
303 molecules have the potential to behave differently than what we observed here and may affect
304 the sorption of the low molecular weight compounds. However, the general patterns of sorption
305 were similar between the two experimental systems examined (the complex bacterial lysates
306 versus the simpler standards mixture) indicating that the effects of the undetected compounds
307 appear to be minor.

308 Organic matter-mineral interactions are complex; typically involving a combination and
309 layers of electrostatic interactions, covalent bonding, hydrogen bonding and hydrophobic
310 bonding resulting in inner-sphere and/ or outer-sphere surface complexes (Kleber et al., 2007;
311 Sutton and Sposito, 2005). Characterizing these specific interactions would require extensive
312 further investigation typically achieved by the use of attenuated total reflectance Fourier
313 transform infrared spectroscopy or x-ray absorption spectroscopy (Arai and Sparks, 2007;
314 Persson and Axe, 2005; Yeasmin et al., 2014). However, predictions can be made on mineral
315 surface interactions based on our experimental conditions and observations made in previous
316 studies.

317 Iron oxides have a variable charge (pH-dependent) surface resulting from the iron metal
318 center and surface hydroxyls. The point of zero charge for Si-free ferrihydrite is 7.6
319 (Schwertmann and Fechter, 1982) so at our experimental $\text{pH} \leq 7.2$ it can be assumed that the
320 aged ferrihydrite has a net positive charge. The positive charge on the iron oxide surface and
321 negative charge of phosphate-containing microbial metabolites and carboxyl groups would

322 induce electrostatic attraction. One proposed mechanism is that phosphate-containing
323 compounds in the bacterial lysate may form phosphate-Fe bonds via a ligand exchange
324 mechanism (by displacing surface hydroxyls), a mechanism observed with goethite (Omoike and
325 Chorover, 2006). However, in many cases, this is usually accompanied by a large increase in pH
326 as hydroxyls are released into solution (Parfitt et al., 1977), which was not observed here,
327 suggesting that this is not the primary mechanism of sorption. Our results agree with previous
328 reports of anionic compounds such as carboxylates sorbing more readily to soil and mineral
329 surfaces (Swenson et al, 2015) with the degree of sorption increasing with the number of
330 dissociable carboxyl groups (Yeasmin et al., 2014). This previous study is also in line with our
331 observation of alanine, phenylalanine and lysine not being preferentially sorbed relative to other
332 carboxyl-containing compounds (Yeasmin et al., 2014). Phenylalanine did sorb slightly better
333 compared to alanine and lysine, potentially due to the presence of the aromatic side-chain.

334

335 ***4.2. Sorption patterns and behavior of microbial metabolites***

336 For individual metabolites, three distinct sorption patterns relative to mineral
337 concentration were observed as shown by figures 1 and 2: linear (sorption steadily increased with
338 mineral concentration), saturation (sorption rapidly increased to 100% with mineral
339 concentration) and on-off-on (sorption at low and high mineral concentrations, but not at
340 medium concentrations). A saturation-type pattern was displayed by all phosphate-containing
341 metabolites as shown by a rapid increase in sorption (at low mineral concentrations) then a
342 plateau at medium-to-high concentrations, presumably as all mineral binding sites (capable of
343 binding these particular metabolites) became occupied at a given mineral concentration. The
344 third pattern, observed with 12 out of the 14 detected amino acids, was the on-off-on pattern with

345 a small amount of sorption occurring only at the lowest and highest mineral concentrations. The
346 detected amino acids represent a nice set of structurally similar compounds that also vary in
347 several key properties, *e.g.* charge and hydrophobicity, and therefore the comparison of the their
348 behavior can provide insight into the experiment as a whole and merit some further discussion.
349 Since our experimental conditions were below the point of zero charge for ferrihydrite, the
350 surface should be slightly net positive initially or at low surface loadings. Not surprisingly
351 therefore, the two amino acids that sorbed 100% at the lowest surface loading of organics, *i.e.* 32
352 mg ferrihydrite, were aspartate and glutamate which are also the only two that are strongly
353 negatively charged at pH 6.8 with pIs of 2.8 and 3.2, respectively. The two that didn't sorb at all
354 at 32 mg ferrihydrite treatment were arginine and lysine which are also the two that are
355 positively charged at pH 6.8 (pIs of 10.8 and 9.7, respectively). The other 10 amino acids are all
356 slightly negative at pH 6.8 (pIs 5.5-6.3), and sorbed less than the negative ones and more than
357 the positive ones, *i.e.* between 20-80% at 32 mg ferrihydrite. This range shows that charge is not
358 the only factor impacting sorption, but is likely a key one. At the highest surface loading of
359 organics (0.5 mg ferrihydrite), the mineral surface is expected to be increasingly less positive or
360 potentially negative and more hydrophobic because of more organics on the surface (Weng et al.,
361 2006), and the result is that the two positive amino acids, lysine and arginine, exhibit sorption
362 (4% and 13%, respectively). Many of the slightly negative amino acid also sorb under these
363 conditions, potentially due to the ferrihydrite surface also being more hydrophobic at high
364 surface loading of organics. For example, tryptophan and phenylalanine, two of the most
365 hydrophobic amino acids, sorb 8% and 9%, respectively. The fact that so many of the amino
366 acids show a minimum at intermediate ferrihydrite concentrations is likely a result of the
367 changing importance of competitive sorption and changing surface characteristics, *e.g.* charge

368 and hydrophobicity as a function of surface loading of organics. These results highlight the
369 situational dependence of organic sorption on minerals surfaces and emphasize the potential of
370 microbial strategies that could change surface behavior in a way that benefits an organism.

371 Overall, our results suggest that in iron oxide-rich soils, metabolites such as ectoine,
372 lysine, uracil and disaccharides (*e.g.* maltose and trehalose) may be readily available for
373 microbial processing and cycling. Many of these compounds are known to be commonly utilized
374 by a variety of microorganisms (Fredrickson et al., 1991). The availability of these favored
375 metabolites is often central to the survival of terrestrial microbes especially in harsh
376 environmental conditions. For example, in addition to being important carbon sources, ectoine
377 and trehalose are common microbial protectants against changes in salinity and temperature
378 (Reina-Bueno et al., 2012).

379

380 ***4.3. Mechanisms of phosphate sorption and exchange with microbial metabolites***

381 Phosphorus (both organic and inorganic forms) plays an essential biogeochemical role for
382 all living organisms and therefore an understanding of its behavior and retention in soils is
383 crucial. Phosphorus behavior is complex and depends on many environmental factors including
384 iron and aluminum oxide content, pH and organic matter composition (Arai and Sparks, 2007).
385 Ferrihydrite, compared to other iron oxides (*e.g.* goethite and hematite), possesses larger and
386 more rapid phosphate sorption properties probably due to its higher surface area density (Wang
387 et al., 2013). When the environmental pH is below the point of zero charge (which was the case
388 for our phosphate experiments), the primary mechanism of phosphate sorption, as with
389 negatively-charged metabolites, is via electrostatic interaction (Arai and Sparks, 2007). The
390 mechanism of (inner-sphere bound) phosphate release from iron oxide surfaces by organic acids

391 is known to occur by two main mechanisms: ligand exchange and ligand-enhanced dissolution of
392 minerals (Johnson and Loeppert, 2006). Here we examined the ability of high-sorbing microbial
393 metabolites to control phosphate bioavailability rather than to determine the mechanism.

394

395 ***4.4. Microbial metabolite release as a potential mechanism to mobilize phosphate***

396 Given the observed sorption of many metabolites onto the mineral, we wondered if some
397 of these displace phosphate. While there is much evidence of plants releasing organic acids to
398 obtain access to limiting nutrients such as phosphate (Gahoonia et al., 2000; Johnson and
399 Loeppert, 2006; Vance et al., 2003), it seems that the role of metabolite release for this purpose
400 by microbes is less understood. Phosphate-solubilizing microbes (bacteria, fungi, actinomycetes
401 and cyanobacteria) are being explored as a means to solubilize phosphate for plant nutrition and
402 such strains can constitute as much as 50% of the total soil bacteria population (Johnson and
403 Loeppert, 2006; Sharma et al., 2013). Production of organic acids and chelation of mineral ions
404 by these compounds, rather than acidification, appears to be a more effective mechanism for
405 phosphate solubilization from iron or aluminum minerals (Barea and Richardson, 2015).
406 However, most research to date has primarily focused on microbial production of organic acids
407 such as gluconate, citrate, succinate and oxalate (Barea and Richardson, 2015; Illmer et al., 2003;
408 Rashid et al., 2004; Whitelaw et al., 1999), rather than on other potential phosphate-solubilizing
409 small molecules.

410 Here, we examined the most sorptive metabolites and found that of the compounds
411 tested, the ones that released the most phosphate into solution were the phosphate-containing
412 metabolites. Although this would not result in a net gain in phosphate for the microbe itself, one
413 can hypothesize that microbes that are less phosphate-dependent may release these compounds

414 for the benefit of symbiotic plants (Zaidi et al., 2009) or microbes. Some non-phosphate
415 metabolites (glutathione and citrate) did displace small amounts of phosphate as indicated in our
416 study. A further area of exploration would be to examine more non-phosphate metabolites such
417 as these for their ability to displace phosphate from ferrihydrite or other minerals. Additionally,
418 exometabolomics studies (Silva and Northen, 2015) would be required to confirm the release of
419 metabolites from microbial isolates in support of possible phosphate- (or other oxyanion-)
420 mobilizing mechanisms.

421

422 **CONCLUSION**

423 Understanding SOM turnover and mineral interactions of this complex pool of small
424 molecules is essential to understanding soil carbon and nitrogen dynamics and these processes
425 greatly influence microbial community activity and structure. Exploring single metabolite or
426 general SOM sorption is difficult to translate to *in situ* conditions, hence our focus was on a
427 microbial metabolite mixture with an iron oxide mineral. Ferrihydrite is a common soil mineral
428 and is known for its large surface area and generally high reactivity. Iron oxides, and ferrihydrite
429 in particular, are important in the creation of organic matter-mineral associations that are thought
430 to impact the long-term stability of carbon in many soil systems and in controlling nutrient
431 concentrations in soils. Our findings reveal that phosphate-containing and dicarboxylate
432 metabolites strongly sorb to the mineral and thus are unlikely to be readily available for SOM
433 cycling and microbial processing in iron oxide-rich environments, but important osmolytes such
434 as ectoine and disaccharides were found to be less sorptive and more available. Furthermore, the
435 highly-sorptive metabolites identified here mobilize phosphate from the iron oxide mineral
436 surface and may allow microbes to gain access to limiting oxyanion nutrients. Overall, these

437 results will aid in our understanding of how specific mineral and chemical factors of a given
438 environment may affect SOM dynamics.

439

440 **ACKNOWLEDGEMENTS**

441 This work was funded by the Office of Science Early Career Research Program (No. DE-
442 AC02-05CH11231), Office of Biological and Environmental Research and P.N. is funded by the
443 Terrestrial Ecosystem Science, Science Focus Area, both of the U.S. Department of Energy
444 under contract to Lawrence Berkeley National Laboratory

445

446 **REFERENCES**

- 447 Alexander, M., 1977. Introduction to Soil Microbiology. John Wiley & Sons, Hoboken, NJ.
- 448 Amon, R.M.W., Fitznar, H.-P., Benner, R., 2001. Linkages among the bioreactivity, chemical
449 composition, and diagenetic state of marine dissolved organic matter. *Limnology and*
450 *Oceanography* 46, 287–297.
- 451 Arai, Y., Sparks, D.L., 2007. Phosphate Reaction Dynamics in Soils and Soil Components: A
452 Multiscale Approach, in: Sparks, D.L. (Ed.), *Advances in Agronomy*. Elsevier Inc., New
453 York, pp. 135–179.
- 454 Barea, J.-M., Richardson, A.E., 2015. Chapter 24. Phosphate Mobilisation by Soil
455 Microorganisms, in: Lugtenberg, B. (Ed.), *Principles of Plant-Microbe Interactions*. Springer
456 International Publishing, Switzerland, pp. 225–234.
- 457 Batjes, N.H., 1996. Total carbon and nitrogen in the soils of the world. *European Journal of Soil*
458 *Science* 47, 151–163.
- 459 Bowen, B.P., Yao, Y., Sun, T., Wang, T., Ruebel, O., Northen, T., 2015. Analysis of

460 metabolomics datasets with high-performance computing and Metabolite Atlases.
461 Metabolites. submitted.

462 Cagnasso, M., Boero, V., Franchini, M.A., Chorover, J., 2010. ATR-FTIR studies of
463 phospholipid vesicle interactions with α -FeOOH and α -Fe₂O₃ surfaces. *Colloids and*
464 *Surfaces B: Biointerfaces* 76, 456–467.

465 Davidson, E.A., Janssens, I.A., 2006. Temperature sensitivity of soil carbon decomposition and
466 feedbacks to climate change. *Nature* 440, 165–173.

467 Fredrickson, J.K., Balkwill, D.L., Zachara, J.M., Li, S-M.W., Brockman, F.J., Simmons, M.A.,
468 1991. Physiological diversity and distributions of heterotrophic bacteria in deep cretaceous
469 sediments of the Atlantic coastal plain. *Applied and Environmental Microbiology* 57, 402-
470 411.

471 Gahoonia, T.S., Asmar, F., Giese, H., Gissel-Nielsen, G., Nielsen, N.E., 2000. Root-released
472 organic acids and phosphorus uptake of two barley cultivars in laboratory and field
473 experiments. *European Journal of Agronomy* 12, 281–289.

474 Giardina, C.P., Ryan, M.G., 2000. Evidence that decomposition rates of organic carbon in
475 mineral soil do not vary with temperature. *Nature* 404, 858–861.

476 Guigue, J., Lévêque, J., Mathieu, O., Schmitt-Kopplin, P., Lucio, M., Arrouays, D., Jolivet, C.,
477 Dequiedt, S., Prévost-Bouré, N.C., Ranjard, L., 2015. Water-extractable organic matter
478 linked to soil physico-chemistry and microbiology at the regional scale. *Soil Biology and*
479 *Biochemistry* 84, 158-167.

480 Heckman, K., Grandy, A.S., Gao, X., Keiluweit, M., Wickings, K., Carpenter, K., Chorover, J.,
481 Rasmussen, C., 2013a. Sorptive fractionation of organic matter and formation of organo-
482 hydroxy-aluminum complexes during litter biodegradation in the presence of gibbsite.

483 *Geochimica et Cosmochimica Acta* 121, 667–683.

484 Heckman, K., Welty-Bernard, A., Vazquez-Ortega, A., Schwartz, E., Chorover, J., Rasmussen,
485 C., 2013b. The influence of goethite and gibbsite on soluble nutrient dynamics and microbial
486 community composition. *Biogeochemistry* 112, 179–195.

487 Hopkins, F.M., Torn, M.S., Trumbore, S.E., 2012. Warming accelerates decomposition of
488 decades-old carbon in forest soils. *Proceedings of the National Academy of Sciences USA*
489 109, 10152–10153.

490 Hopkinson, C.S., Buffam, I., Hobbie, J., Vallino, J., Perdue, M., Eversmeyer, B., Prah, F.,
491 Covert, J., Hodson, R., Moran, M.A., Smith, E., Baross, J., Crump, B., Findlay, S., Foreman,
492 K., 1998. Terrestrial inputs of organic matter to coastal ecosystems: An intercomparison of
493 chemical characteristics and bioavailability. *Biogeochemistry* 43, 211–234.

494 Houghton, R.A., 2007. Balancing the global carbon budget. *Annual Review of Earth and*
495 *Planetary Sciences* 35, 313–347.

496 Illmer, P., Barbato, A., Schinner, F., 2003. Solubilization of hardly-soluble AlPO_4 with P-
497 solubilizing microorganisms. *Soil Biology and Biochemistry* 27, 265–270.

498 Johnson, S.E., Loeppert, R.H., 2006. Role of organic acids in phosphate mobilization from iron
499 oxide. *Soil Science Society of America Journal* 70, 222–234.

500 Judd, K.E., Crump, B.C., Kling, G.W., 2006. Variation in dissolved organic matter controls
501 bacterial production and community composition. *Ecology* 87, 2068–2079.

502 Kaiser, K., Guggenberger, G., 2007. Sorptive stabilization of organic matter by microporous
503 goethite: sorption into small pores vs. surface complexation. *European Journal of Soil*
504 *Science* 58, 45–59.

505 Kaiser, K., Kalbitz, K., 2012. Cycling downwards - dissolved organic matter in soils. *Soil*

506 Biology and Biochemistry 52, 29–32.

507 Kakumanu, M.L., Cantrell, C.L., Williams, M.A., 2013. Microbial community response to
508 varying magnitudes of desiccation in soil: a test of the osmolyte accumulation hypothesis.
509 Soil Biology and Biochemistry 57, 644–653.

510 Kalbitz, K., 2003. Changes in properties of soil-derived dissolved organic matter induced by
511 biodegradation. Soil Biology and Biochemistry 35, 1129–1142.

512 Kalbitz, K., Solinger, S., Park, J.H., Michalzik, B., Matzner, E., 2000. Controls on the dynamics
513 of dissolved organic matter in soils: A review. Soil Science 165, 277–304.

514 Karhu, K., Auffret, M.D., Dungait, J.A.J., Hopkins, D.W., Prosser, J.I., Singh, B.K., Subke, J.-
515 A., Wookey, P.A., Ågren, G.I., Sebastià, M.-T., Gouriveau, F., Bergkvist, G., Meir, P.,
516 Nottingham, A.T., Salinas, N., Hartley, I.P., 2014. Temperature sensitivity of soil respiration
517 rates enhanced by microbial community response. Nature 513, 81–84.

518 Kleber, M., Sollins, P., Sutton, R., 2007. A conceptual model of organo-mineral interactions in
519 soils: self-assembly of organic molecular fragments into zonal structures on mineral
520 surfaces. Biogeochemistry 85, 9–24.

521 Ludwig, M., Achtenhagen, J., Miltner, A., Eckhardt, K.-U., Leinweber, P., Emmerling, C.,
522 Thiele-Bruhn, S., 2015. Microbial contribution to SOM quantity and quality in density
523 fractions of temperate arable soils. Soil Biology and Biochemistry 81, 311–322.

524 Omoike, A., Chorover, J., 2006. Adsorption to goethite of extracellular polymeric substances
525 from *Bacillus subtilis*. Geochimica et Cosmochimica Acta 70, 827–838.

526 Parfitt, R.L., Fraser, A.R., Farmer, V.C., 1977. Adsorption on hydrous oxides. III. Fulvic acid
527 and humic acid on goethite, gibbsite and imogolite. Journal of Soil Science 28, 289–296.

528 Persson, P., Axe, K., 2005. Adsorption of oxalate and malonate at the water-goethite interface:

529 Molecular surface speciation from IR spectroscopy. *Geochimica et Cosmochimica Acta* 69,
530 541–552.

531 Rashid, M., Khalil, S., Ayub, N., Alam, S., Latif, F., 2004. Organic acids production and
532 phosphate solubilization by phosphate solubilizing microorganisms (PSM) under *in vitro*
533 conditions. *Pakistan Journal of Biological Sciences* 7, 187–196.

534 Reina-Bueno, M., Argandoña, M., Salvador, M., Rodríguez-Moya, J., Iglesias-Guerra, F.,
535 Csonka, L.N., Nieto, J.J., Vargas, C., 2012. Role of trehalose in salinity and temperature
536 tolerance in the model halophilic bacterium *Chromohalobacter salexigens*. *PLoS ONE* 7,
537 e33587.

538 Schmidt, M.W.I., Torn, M.S., Abiven, S., Dittmar, T., Guggenberger, G., Janssens, I.A., Kleber,
539 M., Kögel-Knabner, I., Lehmann, J., Manning, D.A.C., Nannipieri, P., Rasse, D.P., Weiner,
540 S., Trumbore, S.E., 2011. Persistence of soil organic matter as an ecosystem property.
541 *Nature* 478, 49–56.

542 Schwertmann, U., Cornell, R. M., 2000. Chapter 8. Ferrihydrite. In: Schwertmann, U., Cornell,
543 R. M. (Eds.), *Iron Oxides in the Laboratory: Preparation and Characterization*. Wiley-VCH
544 Verlag GmbH, Weinheim, Germany, pp. 103-112.

545 Schwertmann, U., Fechter, H., 1982. The point of zero charge of natural and synthetic
546 ferrihydrites and its relation to adsorbed silicate. *Clay Minerals* 17, 471-476.

547 Sharma, S.B., Sayyed, R.Z., Trivedi, M.H., Gobi, T.A., 2013. Phosphate solubilizing microbes:
548 sustainable approach for managing phosphorus deficiency in agricultural soils. *Springer Plus*
549 2, 587.

550 Silva, L.P., Northen, T.R., 2015. Exometabolomics and MSI: deconstructing how cells interact to
551 transform their small molecule environment. *Current Opinion in Biotechnology* 34, 209–

552 216.

553 Sutton, R., Sposito, G., 2005. Molecular structure in soil humic substances: The new view.
554 Environmental Science and Technology 39, 9009–9015.

555 Swenson, T.L., Jenkins, S., Bowen, B.P., Northen, T.R., 2015. Untargeted soil metabolomics
556 methods for analysis of extractable organic matter. Soil Biology and Biochemistry 80, 189–
557 198.

558 Vance, C.P., Uhde-Stone, C., Allan, D.L., 2003. Phosphorus acquisition and use: critical
559 adaptations by plants for securing a nonrenewable resource. New Phytologist 157, 423–447.

560 Vogel, C., Babin, D., Pronk, G.J., Heister, K., Smalla, K., Kögel-Knabner, I., 2014.
561 Establishment of macro-aggregates and organic matter turnover by microbial communities in
562 long-term incubated artificial soils. Soil Biology and Biochemistry 79, 57–67.

563 Wang, X., Liu, F., Tan, W., Li, W., Feng, X., Sparks, D.L., 2013. Characteristics of phosphate
564 adsorption-desorption onto ferrihydrite. Soil Science 178, 1–11.

565 Warren, C.R., 2015. Comparison of methods for extraction of organic N monomers from soil
566 microbial biomass. Soil Biology and Biochemistry 81, 67–76.

567 Weng, L., Van Riemsdijk, W.H., Koopal, L.K., Hiemstra, T., 2006. Adsorption of humic
568 substances on goethite: Comparison between humic acids and fulvic acids. Environmental
569 Science and Technology 40, 7494-7500.

570 Whitelaw, M.A., Harden, T.J., Helyar, K.R., 1999. Phosphate solubilisation in solution culture
571 by the soil fungus *Penicillium radicum*. Soil Biology and Biochemistry 31, 655–665.

572 Yeasmin, S., Singh, B., Kookana, R.S., Farrell, M., Sparks, D.L., Johnston, C.T., 2014. Influence
573 of mineral characteristics on the retention of low molecular weight organic compounds: A
574 batch sorption-desorption and ATR-FTIR study. Journal of Colloid And Interface Science

575 432, 246–257.

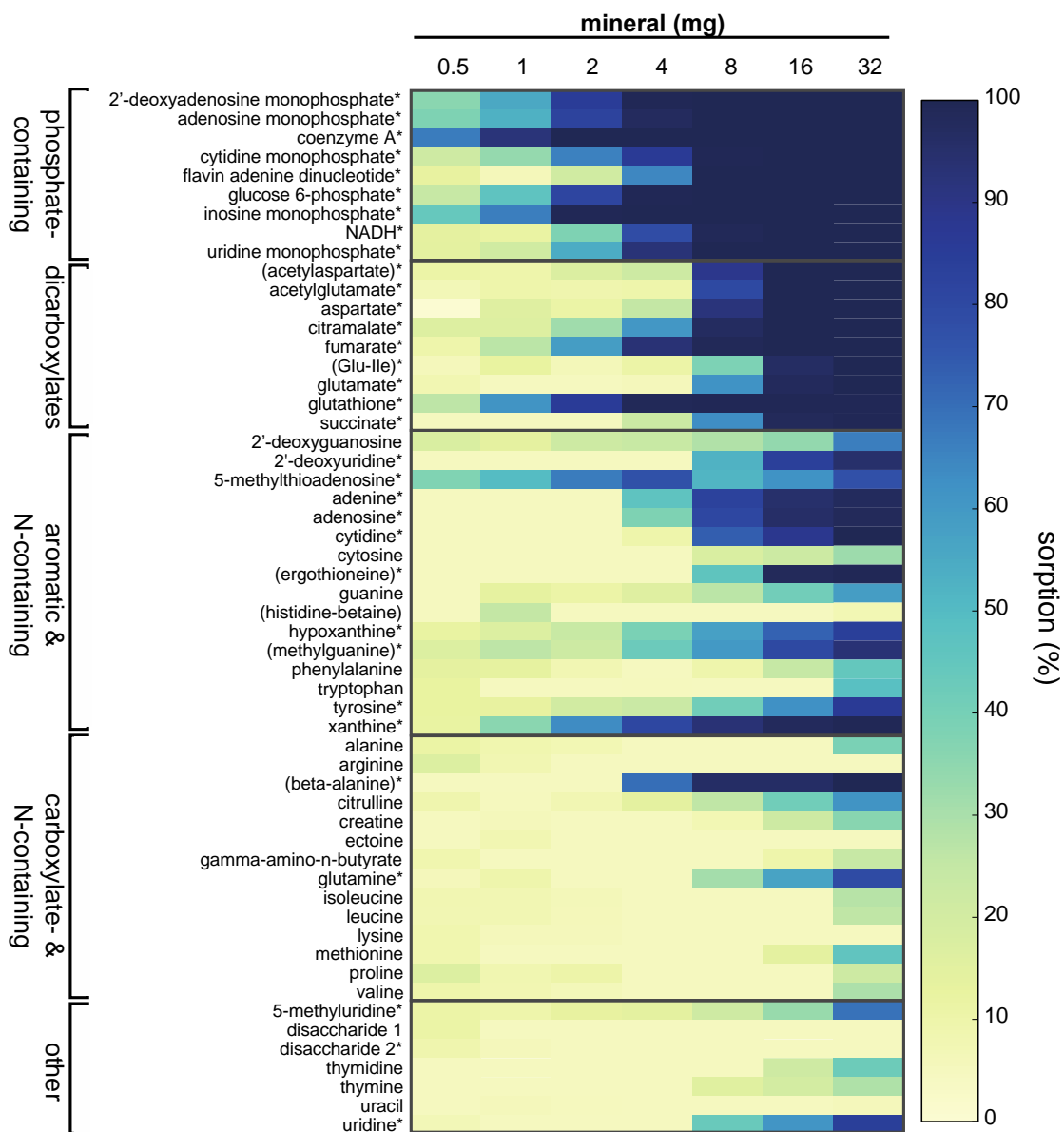
576 Zaidi, A., Khan, M.S., Ahemad, M., Oves, M., Wani, P.A., 2009. Chapter 2. Recent Advances in
577 Plant Growth Promotion by Phosphate-Solubilizing Microbes, in: Khan, M.S., Zaidi, A.,
578 Musarrat, J. (eds.), *Microbial Strategies for Crop Improvement*. Springer-Verlag Berlin
579 Heidelberg, pp. 23–50.

580 Zhou, Q., Maurice, P.A., Carbaniss, S.E., 2001. Size fractionation upon adsorption of fulvic acid
581 on goethite: equilibrium and kinetic studies. *Geochimica et Cosmochimica Acta* 65, 803–
582 812.

583 Zsolnay, A., 1996. Dissolved Humus in Soil Waters, in: Piccolo, A. (Ed.), *Humic Substances in*
584 *Terrestrial Ecosystems*. Elsevier Science B.V., Amsterdam, The Netherlands, pp 171-223.

585

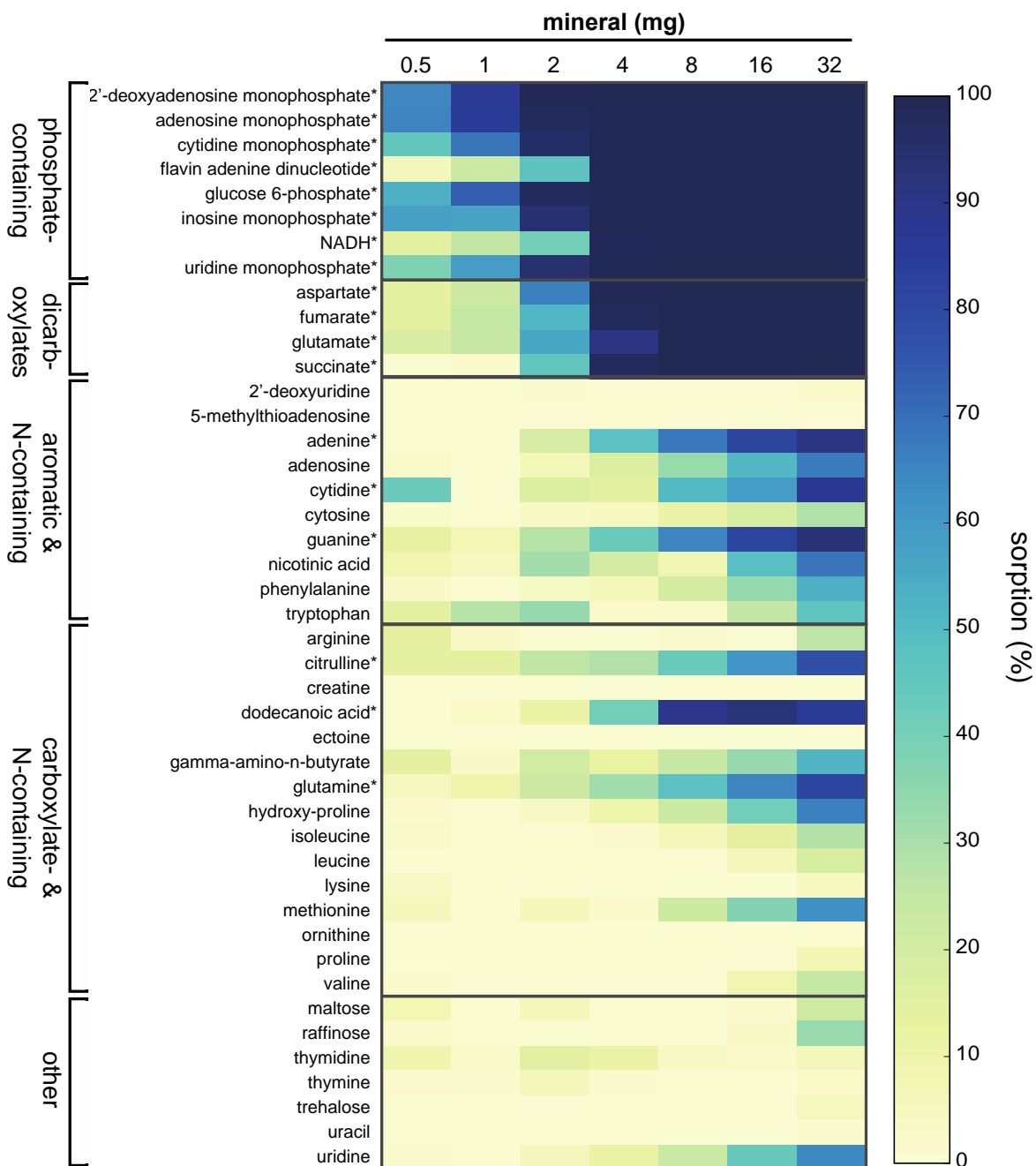
586



589
590 **Figure 1. Mineral sorption of microbial metabolites from *Pseudomonas stutzerii* RCH2**
591 **lysate.** For each metabolite, the percent sorption (relative to the non-mineral control) is displayed
592 as mineral concentration is increased from 0.5 to 32 mg. Phosphate-containing metabolites and
593 dicarboxylates were preferentially sorbed. Metabolites not exhibiting any sorptive activity were
594 ectoine, lysine, disaccharides and uracil. Putatively-identified metabolites are indicated by

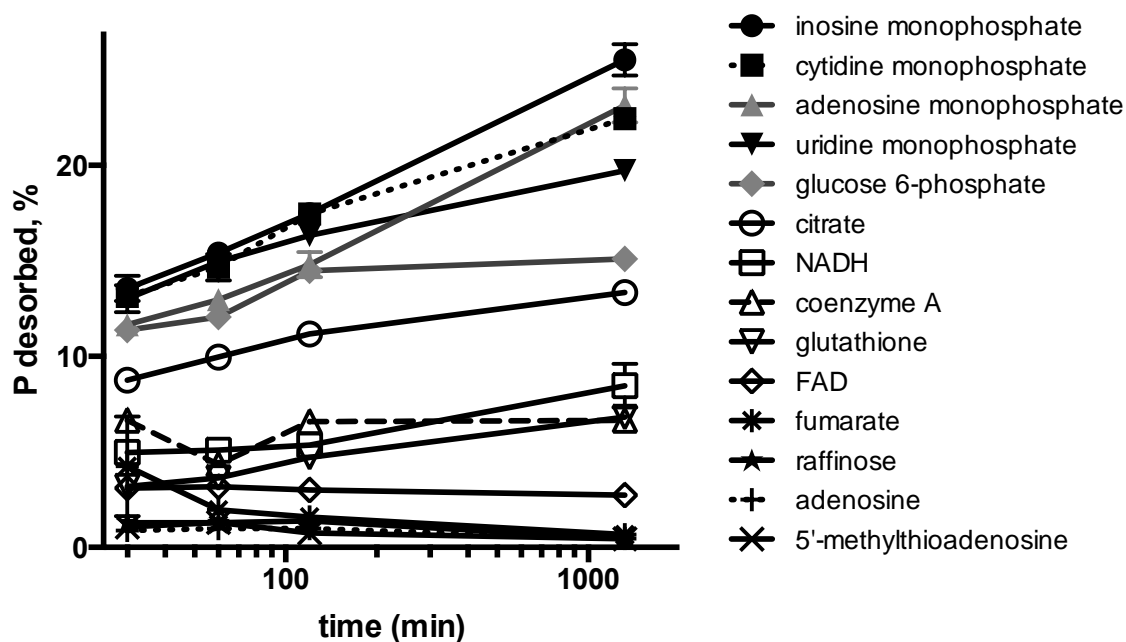
595 parentheses. $n= 5$ for each mineral concentration. $*p < 0.05$ for at least one mineral concentration
 596 relative to the non-mineral control.

597



598

599 **Figure 2. Mineral sorption of the standards mixture.** For each metabolite, the percent sorption
 600 (relative to the non-mineral control) is displayed as mineral concentration is increased (from 0.5
 601 to 32 mg). Phosphate-containing metabolites and dicarboxylates were preferentially sorbed as
 602 observed in the RCH2 bacterial lysate experiment. Metabolites not exhibiting any sorptive
 603 activity include 2'-deoxyuridine, 5-methylthioadenosine, ectoine and ornithine. $n = 5$ for each
 604 mineral concentration. $*p < 0.05$ for at least one mineral concentration relative to the non-
 605 mineral control.



606
 607 **Figure 3. Metabolite-mediated phosphate desorption from the mineral surface.** The mineral
 608 was pre-loaded with phosphate (0.25 mM KH_2PO_4) for 24 h. After metabolites (2.5 mM) were
 609 added, phosphate desorption was monitored for 24 h. Many phosphate-containing metabolites
 610 and glutathione mobilized the most phosphate. $n = 3$ for each metabolite.